# Molecular dynamics studies on thermal behavior of an MFI-type zeolite

K. Yamahara [a],*, K. Okazaki [a], K. Kawamura [b]

[a] Mitsubishi Chemical Corporation, Yokohama Research Center, 1000 Kamoshida-cho, Aoba-ku, Yokohama 227, Japan
[b] Department of Earth and Planetary Sciences, Tokyo Institute of Technology 2-12-1 Ookayama, Meguro-ku, Tokyo 152, Japan

## Abstract

Molecular dynamics (MD) simulations of an MFI-type zeolite have been performed at various temperatures. Crystal structures and vibrational spectra obtained from the simulations were in good agreement with the experimental data. The temperature-induced phase transition between orthorhombic and monoclinic phases, which was already known from experimental measurements, was also reproduced. The potential model used in this study was thus sufficiently applicable to molecular simulations of this type of zeolites. Our MD simulations suggest Pn symmetry for the monoclinic phase instead of experimental $P2_1/n$. A small change in the thermal expansion coefficient was found on the phase transition. In the higher temperature range, another remarkable change was found: the thermal expansion coefficient became negative. This indicates the existence of a higher temperature orthorhombic phase.

## 1. Introduction

Zeolites are generally crystalline aluminosilicates. Their frameworks, composed of interconnected $TO_4(T = Si, Al)$ tetrahedral networks, have numerous molecular dimensional micropores. These channels give rise to characteristic properties of zeolites such as the molecular sieve effect and shape selective catalysis. It is known that zeolite frameworks do not only vibrate thermally, but are also often distorted by phase transitions induced by the presence of sorbed molecules or temperature. It is thus meaningful to model the flexible frameworks in a simulation in order to understand the properties of the zeolites.

MFI-type zeolites have a high Si/Al ratio. A siliceous MFI compound called silicalite is used as a molecular sieve. Other MFI materials called ZSM-5 have been of great interest in recent years because of their high catalytic activity and excellent shape selectivity. They are widely used as industrial catalysts. Several investigations by X-ray diffraction [1–6], as well as by NMR [7,8], indicate that MFI-type zeolites show a reversible phase transition. The phase transition temperature depends on the content of aluminum or other substituted elements [3,4]; the temperature is reported as being about 340 K for H-ZSM-5 [2], while it increases up to 511 K for (Ge)-ZSM-5 [3]. X-ray diffraction showed that the space group symmetries are orthorhombic Pnma [2–6,9,10] and monoclinic $P2_1/n$ [1], above and below the phase transition temperature, respectively.

There are a few simulation studies with respect to this phase transition. Bell et al. [11] reported that lattice energy minimization calculations, per-

formed with the orthorhombic structure of silical-
ite as an initial structure, result in the simulation
of the low-temperature monoclinic phase. Bur-
chart et al. [12] also examined this phase transi-
tion by lattice energy minimization calculations
using their original all-silica force fields. Their
results slightly differ from those of Bell et al. in
that they obtained both phases as energy mini-
mum. Although MD simulations were applied by
Demontis et al. [13], the phase transition could
not be reproduced. They attributed this to the qual-
ity of the potential model.

In the present work, we have carried out MD
simulations of siliceous MFI-type zeolite (silical-
ite) at various temperatures, to investigate its ther-
mal behavior including the phase transition.
Through detailed comparisons between calculated
and experimental properties, it was possible to
check the validity of our potential model for such
a compound and to approach more realistic fea-
tures of zeolites. This study will also provide a
basis for the future study of zeolites with various
structures and compositions.

## 2. Interatomic potential model

Interatomic potential functions consist of Cou-
lombic, short range repulsion, van der Waals
attraction, and Morse potential terms applied only
to the interactions between silicon and oxygen.

$$u_{ij}(r_{ij}) = z_i z_j e^2 / r_{ij} + f_0 (b_i + b_j)$$

$$\exp[(a_i + a_j - r_{ij})/(b_i + b_j)] - c_i c_j / r_{ij}^6$$

$$+ D_{ij} \{ \exp[-2b_{ij}(r_{ij} - r_{ij}^*)]$$

$$- 2\exp[-b_{ij}(r_{ij} - r_{ij}^*)] \} \tag{1}$$

where $r_{ij}$ is an interatomic distance and
$f_0 (= 6.9511 \times 10^{-11} \, \text{N})$ is a constant. Parameters,
$z$, $a$, $b$ and $c$, are for atomic species, and $D_{ij}$, $B_{ij}$
and $r^*_{ij}$ are for Si–O pairs. These parameters,
which were originally determined using the MD
calculations of various silica crystal structures
such as quartz, cristobalite, stishovite, etc. [14],
were slightly modified for zeolite structures using

MD calculations on ZSM-11. All the parameters
are shown in Table 1.

## 3. Molecular dynamics simulations

MD simulations were carried out using the MD
program MXDTRICL [15], developed by one of
us (Kawamura). The Ewald method was applied
for the summations of Coulombic interactions.
The equations of motions were integrated by
means of Verlet's algorithm. The temperatures
and the pressure were controlled by scaling par-
ticle velocities and simulation cell lengths, respec-
tively. In this study, the temperature was varied
over the range of 100–1000 K, and the pressure
was controlled at 1 atm throughout the MD cal-
culations. The simulation cell corresponds to two
crystal unit cells superimposed along c, containing
576 atoms (192 Si and 384 O). Periodic boundary
conditions were adopted. Simulations were started
from one of the experimental structures which
have orthorhombic or monoclinic symmetry,
called ORTHO and MONO, respectively, by Kon-
ingsveld et al. [1,2]. Hereafter we also call the
experimental structures ORTHO and MONO. Ini-
tial simulations were performed to relax the sys-
tem for 5000 steps at 350 K for ORTHO and at
100 K for MONO, with a time step of 0.1 fs
$(0.1 \times 10^{-15} \, \text{s})$. Other runs were always per-
formed with a time step of 2.0 fs $(2.0 \times 10^{-15} \, \text{s})$.
When the temperature was varied, the system was
equilibrated by a 5000-step run. After the equili-
bration, a production run of 5000 steps was per-

Table 1
Parameters of interatomic potential models

| Ion | $z$ | $a$ (Å) | $b$ (Å) | $c$ $(\text{kJ}^{1/2} \, \text{Å}^3 \, \text{mol}^{-1/2})$ |
|-----|-----|---------|---------|---|
| O | −1.2 | 1.905 | 0.150 | 20.0 |
| Si | 2.4 | 0.935 | 0.100 | 0.0 |

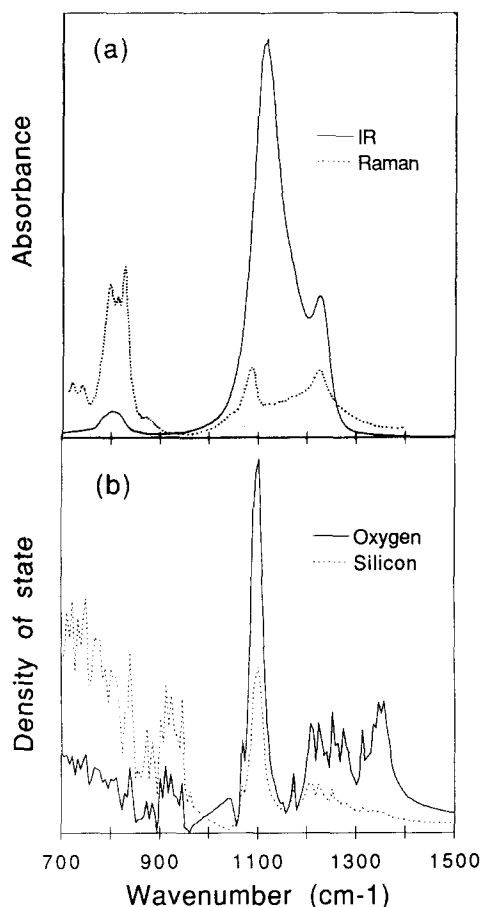| Ion pair | $D \, (10^{-19} \, \text{J})$ | $\beta$ | $r^*$ (Å) |
|----------|------|---------|-----------|
| Si–O | 5.63 | 2.00 | 1.51 |

Fig. 1. Vibrational spectra of silicalite; an experiment at room temperature (a) [16] and a simulation at 350 K (b).

formed, and various time-averaged properties were evaluated. For vibrational spectra, an additional run of 6000 steps was performed.

## 4. Results and discussion

### 4.1. Vibrational spectra

The calculated and experimental [16] vibrational spectra are shown in Fig. 1. The vibrational

spectra were computed as the Fourier transform of the velocity autocorrelation functions of atoms. The calculated vibrational bands are in reasonable agreement with experimental results. This suggests that the oscillatory motion of the framework atoms in the MD simulation is essentially similar to the experimental one.

### 4.2. Crystal structures

In order to check the ability of our model to reproduce orthorhombic and monoclinic phases, MD simulations starting from experimental structures, ORTHO and MONO, were performed at 350 K and at 100 K, respectively. The simulated and experimental lattice parameters are shown in Table 2. The molar volume of the simulation at 100 K seems to be slightly contracted relative to that of MONO, because the temperature of the simulation is lower than that of the experimental measurement of MONO. Lattice parameters obtained from the simulation at 350 K show excellent agreement with those of ORTHO. Thus the lattice parameters of these phases are well reproduced by the MD simulations.

Fig. 2 shows atomic trajectories viewed onto [010] in these MD simulations. The atomic trajectories of the simulation starting from ORTHO are close to atomic positions determined by the X-ray diffraction. The atomic trajectories of the simulation starting from MONO seem to be slightly displaced from experimental positions. The averaged structure of the simulation starting from ORTHO keeps the original orthorhombic Pnma symmetry, while that of the simulation starting from MONO changes its symmetry from the orig-

Table 2
Crystal structures obtained from experiments and simulations

|  | $a$ (Å) | $b$ (Å) | $c$ (Å) | $\alpha$ (°) | $\beta$ (°) | $\gamma$ (°) | $\rho$ (g/cm³) |
|---|---|---|---|---|---|---|---|
| ORTHO[a] | 20.08 | 19.90 | 13.37 | 90 | 90 | 90 | 1.793 |
| MONO[b] | 20.11 | 19.88 | 13.37 | 90.67 | 90 | 90 | 1.792 |
| Simulation from ORTHO at 350 K | 20.08(5) | 19.89(5) | 13.46(2) | 89.97(9) | 90.01(9) | 90.02(5) | 1.781(7) |
| Simulation from MONO at 100 K | 19.94(2) | 19.72(2) | 13.41(1) | 90.68(3) | 90.00(3) | 90.00(2) | 1.817(3) |

[a]Experimental orthorhombic structure at 350 K.
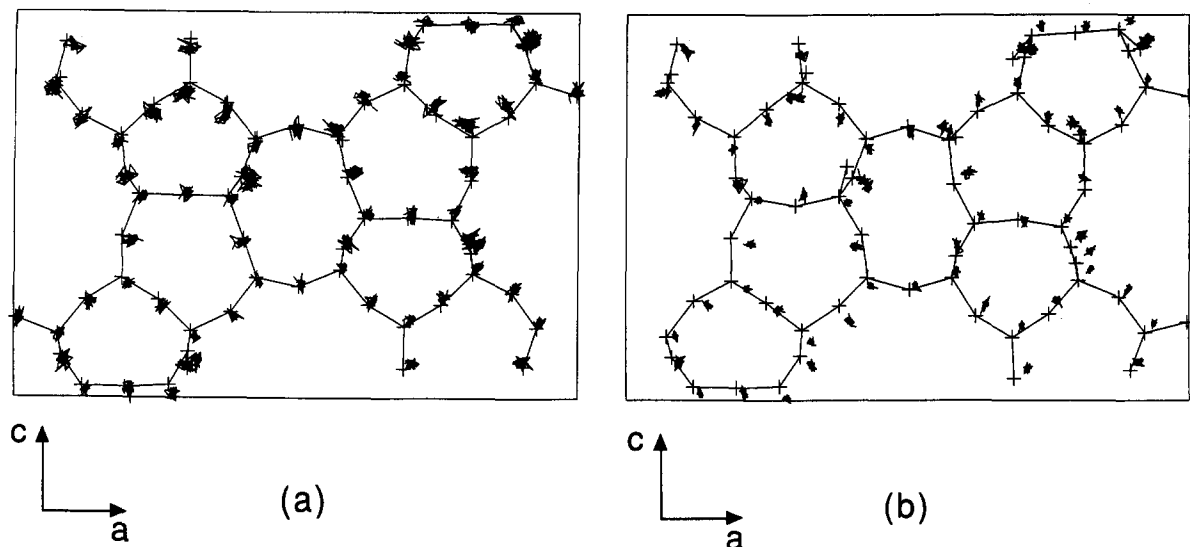[b]Experimental monoclinic structure at room temperature.

Fig. 2. Atomic trajectories viewed onto [010]; a simulation starting from ORTHO at 350 K (a), and from MONO at 100 K (b). The depth along the b axis corresponds to one fifth of the b length of a crystal unit cell. Crosses represent the atomic positions determined by experimental measurements at 350 K for ORTHO and at room temperature for MONO.
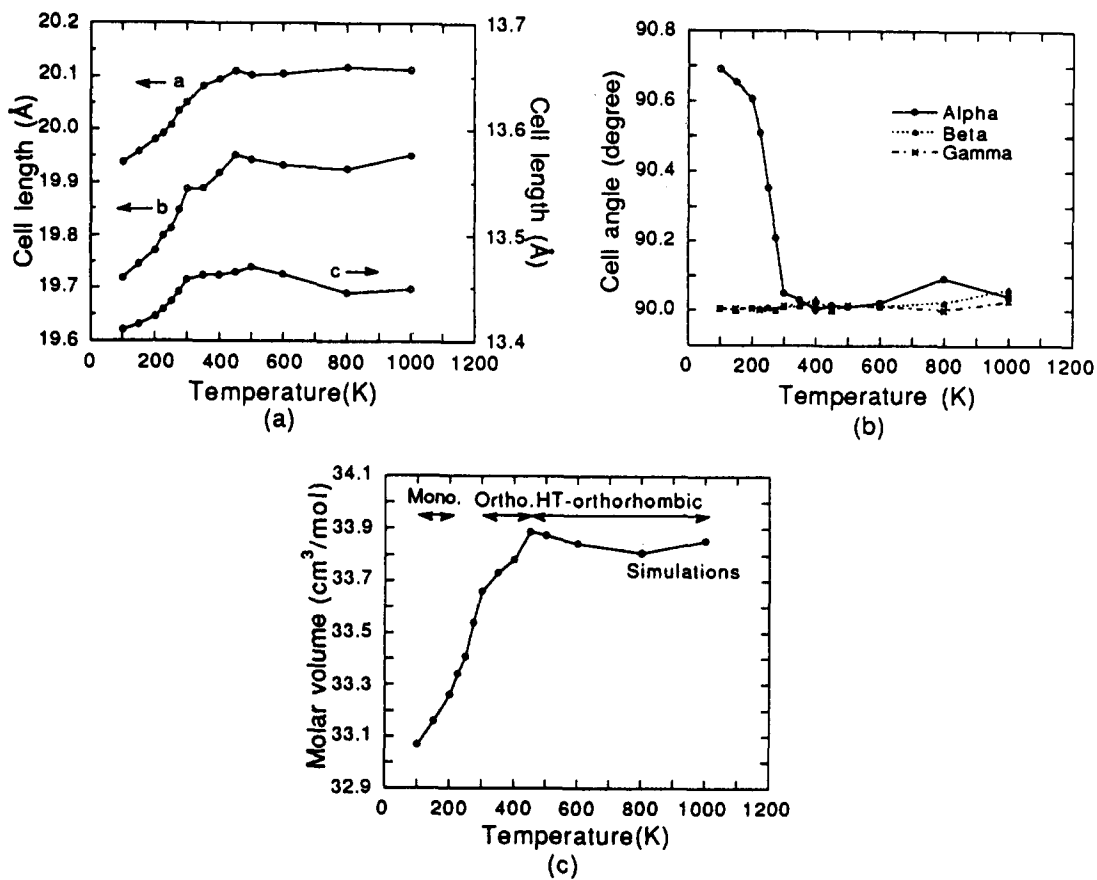


Fig. 3. Temperature dependence of cell parameters (a)(b), and molar volume (c) obtained from the simulation starting from ORTHO.
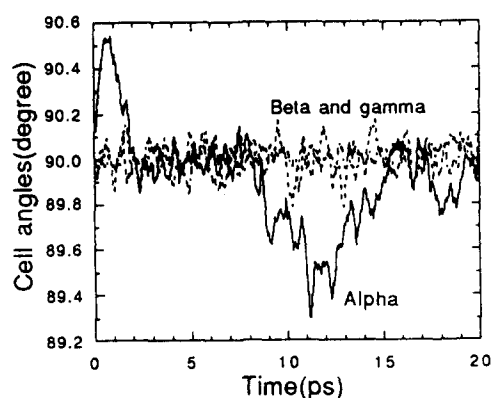
Fig. 4. Cell angle variations obtained from the simulation starting from ORTHO at 275 K.

inal monoclinic $P2_1/n$ to a monoclinic Pn. Thus the orthorhombic structure is well reproduced by MD simulations with respect to lattice parameters, atomic positions, and a space group symmetry, while the monoclinic structure of the MD simulation shows a different symmetry from the experimental one. Nevertheless its lattice parameters are in reasonable agreement with experiment. In the next section, we will discuss this in more detail.

### 4.3. Thermal behavior

MD simulations over the temperature range of 100–1000 K were carried out. Because both the MD simulations starting from ORTHO and MONO give essentially the same results throughout the temperature range, the following data are represented by those of MD simulations starting from ORTHO. Fig. 3 shows the time-averaged temperature dependence of cell parameters and a molar volume. Cell angles (especially angle $\alpha$) show orthorhombic angles at high temperature and monoclinic angles at low temperature. In the temperature range of 225–275 K, a drastic change

in the $\alpha$ angle occurs. It should be noted that in this temperature range, the angle $\alpha$ fluctuates between ca. 90° and ca. 90.6° as shown in Fig. 4. The same results are also obtained from the simulation starting from MONO. The present MD-derived system thus shows a reversible phase transition similar to the experimentally observed one, with respect to the lattice shapes.

The averaged structure has an orthorhombic Pnma symmetry above the transition temperature, and a monoclinic Pn symmetry below, in agreement with the results of Section 4.2. In our MD simulations, the low-temperature monoclinic phase always has Pn symmetry instead of the experimental $P2_1/n$ symmetry. Although further experimental and simulation studies are required, our MD simulations suggest that the phase with monoclinic Pn symmetry may exist below the phase transition temperature. Since most experimental investigations have only been carried out near the transition temperature or at a higher temperature, experimental structural analyses at much lower temperature are desirable.

Table 3 shows the thermal expansion coefficient of each phase estimated from slopes of the curve of Fig. 3c. A small change of the thermal expansion is found on the phase transition; the thermal expansion coefficient above the transition temperature is smaller than that below the transition temperature. This difference has not been confirmed by experimental measurements.

As temperature increases further, the thermal expansion coefficient shows another remarkable change and becomes negative at 450 K, while the space symmetry remains the same. It is known from experimental measurements [17], as well as by MD simulations, that quartz and cristobalite, analogous to zeolites, change into a higher temperature phase with nearly zero or negative values

Table 3
Calculated thermal expansion coefficients

| Initial structure | Monoclinic phase ($K^{-1}$) | Orthorhombic phase ($K^{-1}$) | HT orthorhombic phase ($K^{-1}$) |
|---|---|---|---|
| ORTHO | $5.7 \times 10^{-5}$ | $4.4 \times 10^{-5}$ | $-2.3 \times 10^{-6}$ |
| MONO | $5.2 \times 10^{-5}$ | $4.3 \times 10^{-5}$ | $-4.9 \times 10^{-6}$ |

of thermal expansion coefficients. Our MD simulations may, therefore, suggest that the zeolite shows a phase transition to a higher temperature phase similar to analogs.

## 5. Conclusion

MD simulations of MFI-type zeolite reproduce well the orthorhombic structure above the transition temperature and the monoclinic lattice below the transition temperature. A phase transition similar to the experimentally observed one takes place in the range 225–275 K. The vibrational spectra are also in reasonable agreement with the experimental ones. Thus our MD simulations successfully reproduce some characteristics of the zeolite. This indicates that the potential model used here is sufficiently appropriate for molecular simulations of this type of zeolites. Considering that the potential model was slightly modified from that originally adopted for silica polymorphs except for zeolites, it is expected that the present potential model will be widely effective on silica compounds including zeolites.

In our MD simulations, the low-temperature monoclinic phase always shows Pn symmetry instead of the experimental $P2_1/n$ symmetry. The reason for this disagreement is not clear. Although experimental confirmation and further analyses of the simulations are required, the simulation suggests that a phase with Pn symmetry exists below the transition temperature. The present work also predicts that the thermal expansion coefficient slightly changes on the monoclinic–orthorhombic

phase transition. In addition, it was found that the thermal expansion becomes negative in the higher temperature range ( > 450 K). This suggests the existence of a higher temperature phase similar to that observed for quartz and cristobalite. Experimental investigation of the present results are in progress.

## References

[1] H. van Koningsveld, J.C. Jansen and H. van Bekkum, Zeolites, 10 (1990) 235.

[2] H. van Koningsveld, Acta Cryst., B46 (1990) 731.

[3] A. Lopez, M. Soulard and J.L. Guth, Zeolites, 10 (1990) 134.

[4] H. van Koningsveld, J.C. Jansen and H. van Bekkum, Zeolites, 9 (1987) 243.

[5] H. Strobl, C.A. Fyfe, G.T. Kokotailo and C.T. Pasztor, J. Am. Chem. Soc., 109 (1987) 4733.

[6] E.L. Wu, S.L. Lawton, D.H. Olson, A.C. Rohrman, Jr. and G.T. Kokotailo, J. Phys. Chem., 83 (21) (1979) 2777.

[7] C.A. Fyfe, H. Strobl, G.T. Kokotailo, G.J. Kennedy and G.E. Barlow, J. Am. Chem. Soc., 110 (1988) 3373.

[8] C.A. Fyfe, H. Grondey, Y. Feng and G.T. Kokotailo, J. Am. Chem. Soc., 112 (1990) 8812.

[9] H. Lermer, M. Draeger, J. Steffen and K.K. Unger, Zeolites, 5 (1985) 131.

[10] D.H. Olson, G.T. Kokotailo, S.L. Lawton and W.M. Meier, J. Phys. Chem., 85 (1981) 2238.

[11] R.G. Bell, R.A. Jackson and C.R.A. Catlow, J. Chem. Soc., Chem. Commun., (1990) 782.

[12] E. de Vos Burchart, H. van Bekkum and B. van de Graaf, Zeolites, 13 (1993) 212.

[13] P. Demontis, G.B. Suffritti, S. Quartieri, A. Gamba and E.S. Fois, J. Chem. Soc., Faraday Trans., 87 (1991) 1657.

[14] K. Kawamura, in F. Yonezawa (Editor), Molecular Dynamics Simulations, Springer Verlag, Berlin, 1990, p. 88

[15] K. Kawamura, MXDTRICL, JCPE Newslett., 5 (2) (1993) 30.

[16] D. Scarano, A. Zecchina, S. Bordiga, F. Geobaldo, G. Spoto, G. Petrini, G. Leofanti, M. Padovan and G. Tozzola, J. Chem. Soc., Faraday Trans., 89 (22) (1993) 4123.

[17] R.J. Ackermann and C.A. Sorrell, J. Appl. Cryst., 7 (1974) 461.